

Impact of scale-dependent bias and nonlinear evolution on the ISW

Robert E. Smith

Institute for Theoretical Physics, University of Zurich, Zurich, 8037, Switzerland

I summarize recent results from Smith, Hernandez-Monteagudo & Seljak [1], a study of the impact of nonlinear evolution of gravitational potentials in the LCDM model on the Integrated Sachs-Wolfe (ISW) contribution to the cross-power spectrum of the CMB and a set of biased tracers of the mass. We use a large ensemble of N -body simulations to directly follow the potentials and compare the results to analytic perturbation theory (PT) methods. The PT predictions match our results to high precision for $k < 0.2 h \text{ Mpc}^{-1}$. We analyze the CMB–density tracer cross-spectrum using simulations and renormalized bias PT, and find good agreement. The usual assumption is that nonlinear evolution enhances the growth of structure and counteracts the linear ISW on small scales, leading to a change in sign of the CMB–LSS cross-spectrum at small scales. However, PT analysis suggests that this trend reverses at late times when the logarithmic growth rate $f = d \ln D / d \ln a < 1/2$ or $\Omega_m(z) < 0.3$. Numerical results confirm these expectations and we find nonlinear enhancement of the ISW signal on small scales at late-times. On computing the total contribution to the angular spectrum, we find that nonlinearity and scale dependence of the bias are unable to influence the signal-to-noise of the current and future measurements.

1 Introduction

The temperature fluctuations in the Cosmic Microwave Background (CMB) are directly sensitive to the presence of Dark Energy, through the change in energy that a CMB photon experiences as it propagates through an inhomogeneous Universe with time evolving gravitational potentials, Φ . There are three main processes that give rise to changing potentials: the Integrated Sachs–Wolfe effect [2, ISW], which deals with the linear evolution of potentials; the Rees–Sciama effect [3, RS], which is concerned with the nonlinear evolution of potentials; and the Birkinshaw–Gull effect [4], where time evolving potentials arise due to mass flows. We define the “nonlinear ISW effect” as the sum of all three contributions.

Unfortunately, the nonlinear ISW effect can not be observed directly in the CMB auto-power spectrum, owing to the fact that it affects the low multipoles, where cosmic variance is large. It can however be directly observed by cross-correlating the CMB with tracers of the Large-Scale Structure (hereafter LSS). [5]. This analysis has recently been performed by a number of groups using the WMAP data and several LSS measurements (e.g. SDSS, NVSS, 2MASS), with claims of up to 4σ level detections [6, 7]. In a recent paper, [8] measured the cross-correlation between super-structures and super-voids with the CMB. On stacking the signal they found a $\sim 4.5\sigma$ detection, in multiple WMAP bands, and the sign of which appeared consistent with late-time ISW. This result is very puzzling when one considers signal-to-noise (\mathcal{S}/\mathcal{N}) calculations within the LCDM model. These show that the maximum $\mathcal{S}/\mathcal{N} \sim 7$ for full sky surveys [5]. How then is it possible to obtain such high \mathcal{S}/\mathcal{N} , given the partial sky coverage of current surveys? One proposed solution is that nonlinear evolution of potentials and galaxy bias may increase the \mathcal{S}/\mathcal{N} .

In this study we calculate the impact of nonlinear evolution of gravitational potentials on the angular cross-spectrum between a biased set of density tracers and the CMB. We ask whether such effects influence \mathcal{S}/\mathcal{N} . We pursue a two-pronged attack: our first line of inquiry is analytic, and we use perturbation theory (PT) to predict Φ , and this we do in §2; our second line is to use a large ensemble of N -body simulations to directly follow Φ , and this we do in §3.

2 The ISW effect in nonlinear PT

The ISW effect may be written as [2]:

$$\frac{\Delta T(\hat{\mathbf{n}})}{T_0} = \frac{2}{c^2} \int_{t_{\text{ls}}}^{t_0} dt \dot{\Phi}(\hat{\mathbf{n}}, \chi; t), \quad (1)$$

where $\hat{\mathbf{n}}$ is a unit direction vector on the sphere, Φ is the dimensionless metric perturbation in the Newtonian gauge, which reduces to the usual gravitational potential on small scales, the ‘over dot’ denotes a partial derivative with respect to the coordinate time t from the FLRW metric, χ is the comoving radial geodesic distance $\chi = \int c dt/a(t)$, and so may equivalently parameterize time. t_0 and t_{ls} denote the time at which the photons are received and emitted (i.e. last scattering), respectively, c is the speed of light and $a(t)$ is the scale factor.

The rate of change of Φ can be calculated from Poisson’s equation ($\nabla^2 \Phi = 4\pi G \bar{\rho} \delta a^2$):

$$\dot{\Phi}(\mathbf{k}, a) = \frac{3}{2} \Omega_{m0} \left(\frac{H_0}{k} \right)^2 \left[\frac{H(a)}{a} \delta(\mathbf{k}, a) - \frac{\dot{\delta}(\mathbf{k}, a)}{a} \right]. \quad (2)$$

Thus we require knowledge of the time evolution of δ and its growth rate $\dot{\delta}$.

The collapse of cosmic structures can be followed into the nonlinear regime using perturbation theory (PT). The solutions for δ in Fourier space may be written [9]:

$$\delta(\mathbf{k}, a) = \sum_{n=1}^{\infty} [D(a)]^n \delta_n(\mathbf{k}, a_0); \quad \delta_n(\mathbf{k}) \equiv \int \frac{\prod_{i=1}^n \{d^3 q_i \delta_1(\mathbf{q}_i)\}}{(2\pi)^{3n-3}} \delta^D(\mathbf{k} - \mathbf{q}_1 - \dots - \mathbf{q}_n) F_n^{(s)}(\mathbf{q}_1, \dots, \mathbf{q}_n), \quad (3)$$

where $\delta_1(\mathbf{q}_i)$ represents an initial field at wavenumber \mathbf{q}_i , and the quantities $F_n^{(s)}(\mathbf{q}_1, \dots, \mathbf{q}_n)$ represent the standard PT interaction kernels, symmetrized in all of their arguments. We may obtain the time rate of change of the fluctuation by simply differentiating the above,

$$\dot{\delta}(\mathbf{k}, a) = f(a) H(a) \sum_{n=1}^{\infty} n [D(a)]^n \delta_n(\mathbf{k}, a_0), \quad (4)$$

where $f(a) \equiv d \log D(a) / d \log a$. Inserting Eqs (3) and (4) into Eq. (2), we find

$$\dot{\Phi}(\mathbf{k}, a) = \frac{3}{2} \Omega_{m0} \left(\frac{H_0}{k} \right)^2 \frac{H(a)}{a} \sum_{n=1}^{\infty} [1 - n f(a)] [D(a)]^n \delta_n(\mathbf{k}, a_0). \quad (5)$$

Consider linear theory, $n = 1$: for the case $\Omega = 1$, $f(a) = 1$ and potentials do not change with time and there is no ISW effect. However, for LCDM $f(a) \approx \Omega_m^{0.6}$, and so $1 - f(a) \geq 0$. Thus $\dot{\Phi}(\mathbf{k}, a) > 0$ for an overdensity, and potentials decay at late times in linear theory. Consider now the nonlinear theory, $n > 1$: we immediately see that there are critical times in the LCDM model and that these are dictated by the sign of the bracket $[1 - n f(a)]$. For $n = 2$ we have $1 - 2f(a) < 0$ for $a < a_{\text{RS}}$, and $1 - 2f(a) > 0$ for $a > a_{\text{RS}}$, and we call a_{RS} the Rees-Sciama time. For $a < a_{\text{RS}}$ nonlinear evolution enhances the growth of potential wells, but for $a > a_{\text{RS}}$ it augments their decay. Thus it is theoretically possible to boost the late-time ISW effect.

3 The ISW effect in N -body simulations

We use the Zürich Horizon, “zHORIZON”, simulations to study the ISW. These are a large ensemble of pure CDM N -body simulations ($N_{\text{sim}} = 30$). In this study we use the first 8 simulations, since these have 11 snapshots logarithmically spaced in the expansion factor from $z = 1$ to 0, giving good time sampling. Each numerical simulation was performed using the publicly

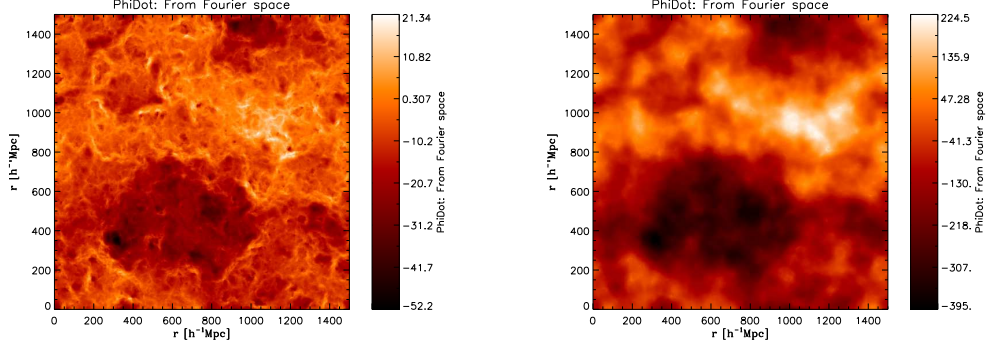


Figure 1: Evolution of $\dot{\Phi}$ in a slab of thickness $\Delta x = 100 h^{-1} \text{Mpc}$. Left $z = 10$ and right $z = 0$.

available `Gadget-2` code [10], and followed the nonlinear evolution under gravity of $N = 750^3$ equal mass particles in a cube of length $L = 1500 h^{-1} \text{Mpc}$. The cosmological parameters are: $\{\Omega_{m0} = 0.25, \Omega_{\Lambda} = 0.75, \sigma_8 = 0.8, n_s = 1.0, h = 0.72\}$, where these are: density parameters in matter and vacuum energy; power spectrum normalization and spectral index; Hubble parameter. Dark matter halo catalogs were generated using the FoF algorithm, and the minimum number of particles for which an object was considered bound was 30. This gave haloes with $M > 1.5 \times 10^{13} M_{\odot}/h$ [for more details see 11].

Considering again Eq. (2) we see that in order to measure the ISW in simulations we need to be able to estimate δ and $\dot{\delta}$. The first is straightforward. The second can be obtained from the continuity equation: $\dot{\delta}(\mathbf{x}) = -\nabla \cdot [1 + \delta(\mathbf{x})] \mathbf{v}(\mathbf{x})/a = -\nabla \cdot \mathbf{p}(\mathbf{x})/a$. In Fourier space this becomes, $\dot{\delta}_k = i\mathbf{k} \cdot \mathbf{p}_k/a$, which may easily be computed [see 1, for details]. Figure 1 presents a visual representation of the ISW effect in the simulations.

4 Results: CMB-LSS angular cross-power spectrum

Under the Limber approximation the CMB-LSS angular cross-power spectrum ($C_l^{\text{h}T}$) is [1]:

$$C_l^{\text{h}T} \approx \int_0^{\chi_{\text{max}}} d\chi \frac{2a}{c^3} \Pi_{ij}(\chi) P_{\text{h}\dot{\Phi}} \left(k = \frac{l}{D_A(\chi)}, \chi \right) \frac{1}{\chi^2}, \quad (6)$$

where $P_{\text{h}\dot{\Phi}} \equiv V_{\mu} \langle \delta_{\text{h}}(\mathbf{k}) \delta_{\dot{\Phi}}(-\mathbf{k}) \rangle$ is the 3D cross-power spectrum between halo density fluctuations δ_{h} and $\dot{\Phi}$. In Eq. (6), we have included the weight function Π_{ij} , which for a mass-selected survey of clusters would have the form:

$$\Pi_{ij}(\chi) \equiv 4\pi D_A^2(\chi) \Theta_{ij}(\chi) \int_{M_{\text{min}}}^{\infty} dM \frac{n(M, \chi)}{N_{\text{TOT}}(\chi_i, \chi_j)}, \quad (7)$$

where D_A is the comoving angular diameter distance and $n(M, \chi)$ the cluster mass function. $N_{\text{TOT}}(\chi_i, \chi_j) = \int_{\chi_i}^{\chi_j} d\chi 4\pi D_A^2(\chi) \int_{M_{\text{min}}}^{\infty} dM n(M; \chi)$, is the total number of clusters above mass M_{min} . The redshift shell is selected using the top-hat function: $\Theta_{ij}(\chi) \equiv [\Theta(\chi - \chi_i) - \Theta(\chi - \chi_j)]$, with Θ the Heaviside step function.

Figure 2 presents the results for $C_l^{\text{h}T}$ between the CMB and group scale dark matter haloes (left panel) and cluster mass haloes (right panel). In each case we show the results for 5 narrow bins in redshift, with $\Delta z = 0.2$. We find that on scales $l < 100$ the departures from linear theory are small $< 10\%$, and are characterized by a small amplification of the signal, followed by a strong suppression. The departures appear small when compared to the cosmic variance, which is dominated by the C_l^{TT} spectrum.

We next investigated the \mathcal{S}/\mathcal{N} for $C_l^{\text{h}T}$ and found good agreement with linear theory expectations: the presence of bias effectively cancels out in the \mathcal{S}/\mathcal{N} expression and leads to

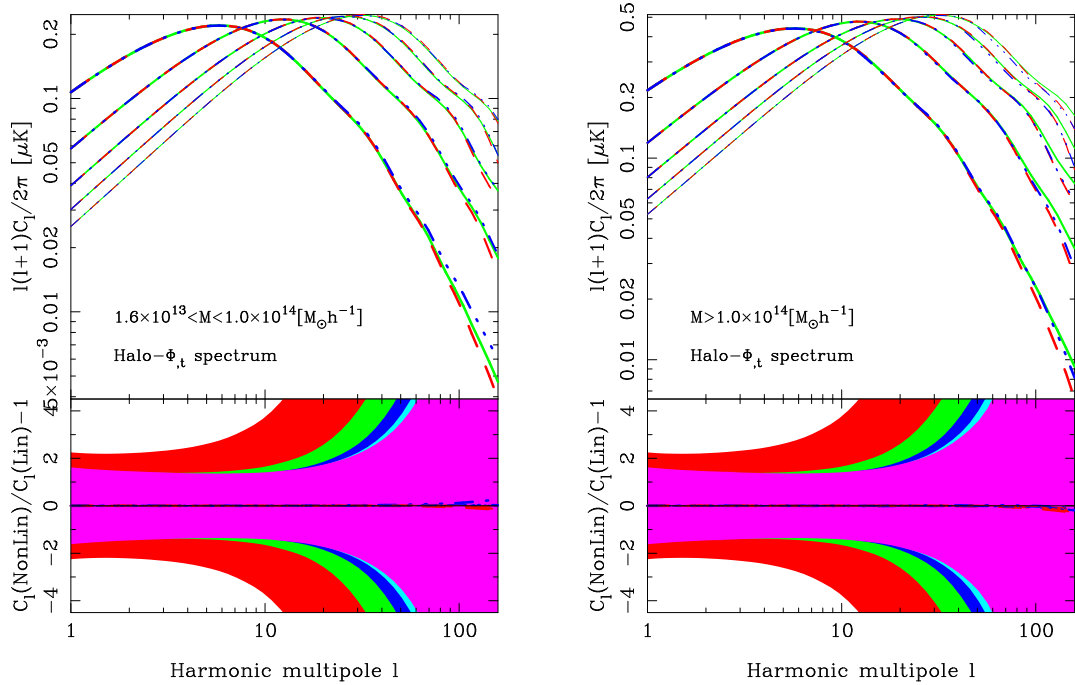


Figure 2: Angular cross-power spectrum of ISW effect and haloes as a function of spherical harmonic multipole l . *Left panel:* results for group-scale dark matter haloes. *Right panel:* results for the cluster-scale haloes. In each panel we show results for 5 equally spaced bins in redshift over the range: $z = [0.0, 1.0]$. The predictions are differentiated by line thickness: thick lines – low redshift; thin lines – high. The line styles denote: linear theory – solid green line; nonlinear PT – red dash line; bi-cubic spline fit to the simulation data – blue triple-dot dash line. Top sections of each panel give the absolute power, and the lower sections the ratio with respect to linear theory. The shaded regions represents the $1\text{-}\sigma$ error domains per multipole of the linear cross-spectra, where the central redshifts $z \in \{0.1, 0.3, 0.5, 0.7, 0.9\}$, correspond to the colors (red, green, blue, cyan, magenta).

negligible changes in the cross-correlation detectability. In fact, through the increased Poisson noise of the biased sample, there was a small reduction in the \mathcal{S}/\mathcal{N} , relative to that for the dark matter–CMB cross-correlation.

5 Conclusions

We therefore conclude that the current power spectrum analyses of [7] and [6] are not affected by nonlinear density evolution or scale-dependent bias and that these do not influence the detectability of the ISW-LSS cross-correlation. We are also led to believe that the results from [8] are unlikely to be explained by nonlinear biasing effects in the Λ CDM model. Whether there remain systematic errors in the CMB data associated with point sources or whether this is an exciting detection of new physics remains an open question.

Acknowledgments: RES was supported by a Marie Curie Reintegration Grant and the Swiss National Foundation under contract 200021-116696/1 and WCU grant R32-2008-000-10130-0.

References

- [1] R. E. Smith, C. Hernández-Monteagudo, and U. Seljak. Impact of scale dependent bias and nonlinear structure growth on the integrated Sachs-Wolfe effect: Angular power spectra. *Phys. Rev. D.* , 80(6):063528–+, September 2009.
- [2] R. K. Sachs and A. M. Wolfe. Perturbations of a Cosmological Model and Angular Variations of the Microwave Background. *Astrophys. J.* , 147:73–+, January 1967.
- [3] M. J. Rees and D. W. Sciama. Larger scale Density Inhomogeneities in the Universe. *Nature (London)* , 217:511–+, February 1968.
- [4] M. Birkinshaw and S. F. Gull. A test for transverse motions of clusters of galaxies. *Nature (London)* , 302:315–317, March 1983.
- [5] R. G. Crittenden and N. Turok. Looking for a Cosmological Constant with the Rees-Sciama Effect. *Physical Review Letters*, 76:575–578, January 1996.
- [6] T. Giannantonio, R. Scranton, R. G. Crittenden, R. C. Nichol, S. P. Boughn, A. D. Myers, and G. T. Richards. Combined analysis of the integrated Sachs-Wolfe effect and cosmological implications. *Phys. Rev. D.* , 77(12):123520–+, June 2008.
- [7] S. Ho, C. Hirata, N. Padmanabhan, U. Seljak, and N. Bahcall. Correlation of CMB with large-scale structure. I. Integrated Sachs-Wolfe tomography and cosmological implications. *Phys. Rev. D.* , 78(4):043519–+, August 2008.
- [8] B. R. Granett, M. C. Neyrinck, and I. Szapudi. An Imprint of Superstructures on the Microwave Background due to the Integrated Sachs-Wolfe Effect. *Astrophys. J. Lett.* , 683:L99–L102, August 2008.
- [9] F. Bernardeau, S. Colombi, E. Gaztañaga, and R. Scoccimarro. Large-scale structure of the Universe and cosmological perturbation theory. *Phys. Rep.* , 367:1–3, September 2002.
- [10] V. Springel. The cosmological simulation code GADGET-2. *Mon. Not. R. Astron. Soc.* , 364:1105–1134, December 2005.
- [11] R. E. Smith. Covariance of cross-correlations: towards efficient measures for large-scale structure. *Mon. Not. R. Astron. Soc.* , pages 1337–+, September 2009.